ISSN: 0067-2904

Ground State Structure of Helium and Phosphorus Isotopes using the Radial Wave Functions of Harmonic-Oscillator and Hulthen Potentials

Ameen M. Hameed*, Arkan R. Ridha
Department of Physics, College of Science, University of Baghdad, Baghdad-Iraq

Received: 14/4/2022 Accepted: 29/2/2022 Published: 30/5/2023

Abstract

The ground state density distributions and electron scattering Coulomb form factors of Helium (^{4,6,8}He) and Phosphorate (^{27,31}P) isotopes are investigated in the framework of nuclear shell model. For stable (^{4}He) and (^{31}P) nuclei, the core and valence parts are studied through Harmonic-oscillator (HO) and Hulthen potentials. Correspondingly, for exotic (^{6,8}He) and (^{27}P) nuclei, the HO potential is applied to the core parts only, while the Hulthen potential is applied to valence parts. The parameters for HO and Hulthen are chosen to reproduce the available experimental size radii for all nuclei under study. Finally, the CO component of electron scattering charge form factors are also investigated. Unfortunately, there is no analytic solution to the Hulthen potential except for the *s* states which are harnessed to the current calculation.

Keywords: exotic nuclei, size radii, density distributions, electron scattering charge form factors, shell model, Helium isotopes, phosphorate isotopes, Hulthen potential.
PACS number(s): 21.10.ft, 21.10Gv, 21.60Cs, 25.30Bf

تركيب الحالة الارضية لنظائر الهيليوم و الفسفور باستخدام الدوال الموجة الشعاعية لجهد المتذبذب التوافقي وجهد هالثين

امين مطاع حميد*، أركان رفعه رضا
قسم الفيزياء، كلية العلوم، جامعة بغداد، بغداد، العراق

الخلاصة:

تم تحقيق توزيعات كثافة الحالة الأرضية وعوامل التشكيل الشحنية للاستطارة الإلكترونية المرنة لنظائر الهيليوم (^{4,6,8}He) ونظائر الفوسفور (^{27,31}P) في إطار انموذج القشرة النووي. بالنسبة لجميع الانوية المذكورة سلفا تحت الدراسة، تمت دراسة اجزاء القلب لها من خلال استخدام الدوال الموجية لجهد المتذبذب التوافقي بينما اجزاء التكافؤ فتمت دراستها من خلال جهد هالثين. تم اختيار معلمات جهد المتذبذب التوافقي ومعلمات جهد هالثين بحيث تولد انصاف الاقطار النووية التجريبية المتوفرة. أخيرًا، تم أيضًا تحقيق مركبة C0 لعوامل التشكيل الشحنية للاستطارة الإلكترونية المرنة. نظرا لعدم وجود حل تحليلي لجهد هالثين، ووجود فقط حل تحليلي لحالات s ، تم اعتماد المدار 1s وتسخيرها في الحسابات الحالية لدراسة اجزاء التكافؤ لجميع الانوية تحت الدراسة.

*Email: ameenalnaimy@gmail.com

Introduction

The cornerstone for the correct computation of nuclear bulk properties is the correct selection of the nuclear mean field leading to satisfied results in comparison with experimental data [1]. Such radial wave functions (WF) obtained from such improved mean fields are not easy to handle; the numerical solution is the main drawback [2]. The Harmonic-oscillator wave functions (HOWFs) do not give satisfactory results since they are mainly characterized by Gaussian downfall behavior at large r [3,4,5]. Therefore, one has to adopt modifications to improve such shortcomings. Hamoudi et al.[6] and Radhi et al.[7] applied two HO size parameters to study some exotic nuclei. The transformed HOWFs (THO) in the local scale transformation were successfully used to study stable and exotic nuclei [8,9]. Besides, in the studies of Ridha [10] and Noori and Ridha[11], the Woods-Saxon potential gave very good results for both stable and exotic nuclei.

In the present work, , the use of HO and Hulthen radial WFs were used to study the density distributions and elastic charge form factors for electron scattering of Helium (^{4,6,8}He) and Phosphorate (^{27,31}P) isotopes.

Theoretical Formulations

The radial differential equation of Schrödinger equation is given by [12]:

$$\frac{1}{r^2}\frac{d}{dr}\left(r^2\frac{d\emptyset_{nlj,t_z}(r)}{dr}\right)+\frac{2\mu_{cm_{t_z}}}{\hbar^2}\left[E_{t_z}-\frac{l(l+1)\hbar^2}{2mr^2}-U(r)\right]\emptyset_{nlj,t_z}(r)=0 \qquad (1)$$

Where: μ, $\hbar$, n , l , j and t_z ($t_z=\frac{1}{2}$ for proton and $t_z=-\frac{1}{2}$ for neutron) represent reduced mass ($\mu_{cm_{t_z}}=\frac{m_{t_z}m_c}{A}$), Planck's constant, principle, orbital, total spin and total isospin for single nucleon, respectively. Where $E_{t_z}=-S_{t_z}$ (E_{t_z} and S_{t_z} are the binding energy and separation energy of single proton or neutron). $U(r)$ represents the nuclear central potential given for Hulthen of the form [13]:

$$U(r)=U^H_{cm_{t_z}}(r)=\frac{V_{0,t_z}}{\left(e^{\beta_{t_z}r}-1\right)} \qquad (2)$$

β_{t_z} is related to the range of the potential $\left(\beta_{t_z}=\frac{1}{R}\right)$ and V_0 represents the depth of the potential. The solution to Eq. (1) can be expressed analytically for s state only [13,14]:

$$\emptyset_{nlj,t_z}(r)=\frac{S_{i,t_z}(r)}{r}\,Y_{00}(\hat{r}) \qquad (3)$$

$S_i(r)$ and $Y_{00}(\hat{r})$ represent the radial form of Weinberg states and spherical harmonics, respectively. $S_i(r)$ is given by [13,14]:

$$S_{i,t_z}(r)=e^{-\kappa_{t_z}r}\sum_{j=0}^{i}a^{(i)}_{j,t_z}e^{-j\beta_{t_z}r} \qquad (4)$$

$a^{(i)}_{j,t_z}$ satisfies the condition and the recurrence relation given by [13,14]:

$$\sum_{j=0}^{i}a^{(i)}_{j,t_z}=0 \qquad (5)$$

and

$$\alpha^{(i)}_{j+1,t_z}=\alpha^{(i)}_{j,t_z}\left(\frac{j\omega_{1,t_z}-\omega_{i,t_z}+j(j-1)}{(j+1)\left(j+\omega_{1,t_z}\right)}\right) \qquad (6)$$

where

$$\omega_{i,t_z} = -\alpha_{i,t_z}\left(\frac{2\mu_{cm_{t_z}}V_{0,t_z}}{\hbar^2\beta_{t_z}^2}\right) \tag{7}$$

The Weinberg state parameters (α_{i,t_z}) are given by [13,14]:

$$\alpha_{i,t_z} = i\left(\frac{2\kappa_{t_z}+i\beta_{t_z}}{2\kappa_{t_z}+\beta_{t_z}}\right) \tag{8}$$

For $1s_{\frac{1}{2}}$ state the $\emptyset_{1s_{\frac{1}{2}},t_z}(r)$ in Eq. (3) can be simplified with the aid of Eq. (4-8) to:

$$\emptyset_{1s_{\frac{1}{2}},t_z}(r) = \frac{\sqrt{2\kappa_{t_z}(\kappa_{t_z}+\beta_{t_z})(2\kappa_{t_z}+\beta_{t_z})}}{\beta_{t_z}}\frac{e^{-\kappa_{t_z}r}}{r}\left[1-e^{-\beta_{t_z}r}\right]Y_{00}(\hat{r}) \tag{9}$$

κ_{t_z} stands for wave number and it is related to the binding energy of the single proton (neutron) by the following expression:

$$\kappa_{t_z}^2 = \frac{2\mu_{cm_{t_z}}S_{t_z}}{\hbar^2} \tag{10}$$

The depth of the potential has a relationship with β_{t_z} and κ_{t_z} by the following formula:

$$V_{0,t_z} = -\frac{\hbar^2\beta_{t_z}^2}{2\mu_{cm_{t_z}}}\left(1+\frac{2\kappa_{t_z}}{\beta_{t_z}}\right) \tag{11}$$

The radial WF of HO potential, where $U(r) = -V_0 + \frac{1}{2}m_{t_z}\omega^2r^2$, the solution to Eq. (1) is given by [15]:

$$R_{nl}(r,b_{t_z}) = \frac{1}{(2l+1)!!}\left[\frac{2^{l-n+3}(2n+2l-1)!!}{\sqrt{\pi}b_{t_z}^3(n-1)!}\right]^{\frac{1}{2}}\left(\frac{r}{b_{t_z}}\right)^l e^{-\frac{r^2}{2b_{t_z}^2}}\sum_{k=0}^{n-1}(-1)^k\frac{(n-1)!\,2^k(2l+1)!!}{(n-k-1)!\,k!\,(2l+2k+1)}\left(\frac{r}{b_{t_z}}\right)^{2k} \tag{12}$$

Where b_{t_z} represents the HO size parameter for neutrons or protons.

The density distributions of protons and neutrons for neutron rich isotopes can be written as:

$$\rho_p(r) = \tfrac{1}{4\pi}\textstyle\sum_{c\in core} n_{c,p}\left|R_{n_cl_c}(r,b_p)\right|^2 \tag{13}$$

$$\rho_n(r) = \frac{1}{4\pi}\sum_{c\in core} n_{c,n}\left|R_{n_cl_c}(r,b_n)\right|^2 + \frac{1}{4\pi}n_{v,n}\left|\emptyset_{1s_{\frac{1}{2}},n}(r)\right|^2 \tag{14}$$

In Eqs.(13) and (14), n_{c,t_z} represents the number of protons(neutrons) in the shell c within the core (c stands for the quantum numbers, n and l). $n_{v,n}$ represents the number of neutron(s) in the valence part.

The density distributions of protons and neutrons for proton rich isotopes can be written as:

$$\rho_n(r) = \frac{1}{4\pi}\sum_{c\in core} n_{c,n}\left|R_{n_cl_c}(r,b_n)\right|^2 \tag{15}$$

$$\rho_p(r) = \frac{1}{4\pi}\sum_{c\in core} n_{c,p}\left|R_{n_cl_c}(r,b_p)\right|^2 + \frac{1}{4\pi}n_{v,p}\left|\emptyset_{1s_{\frac{1}{2}},p}(r)\right|^2 \tag{16}$$

Where $n_{v,p}$ represents the number of neutron (s) in the valence part.

The density distributions of protons and neutrons for stable ^{4}He and ^{31}P nuclei can be written as:

$$\rho_{t_z}(r) = \frac{1}{4\pi}\sum_{c\in core} n_{c,t_z}\left|R_{n_c l_c}(r,b_{t_z})\right|^2 + \frac{1}{4\pi} n_{v,t_z}\left|\emptyset_{1s_{\frac{1}{2}},t_z}(r)\right|^2 \quad (17)$$

The CDD (charge density distribution) can be accounted by folding the point proton and neutron density distribution to the CDD of single proton and neutron[16]:

$$\rho_{ch}(r) = \rho_{ch,p}(r) + \rho_{ch,n}(r) \quad (18)$$

where

$$\rho_{ch,p}(r) = \int \rho_p(r)\rho_{pr}(\boldsymbol{r}-\boldsymbol{r}')d\boldsymbol{r}' \quad (19)$$

and

$$\rho_{ch,n}(r) = \int \rho_{J=0,n}(r)\rho_{neu}(\boldsymbol{r}-\boldsymbol{r}')d\boldsymbol{r}' \quad (20)$$

the CDD of single proton ($\rho_{pr}(\vec{r})$) and neutron($\rho_{neu}(\vec{r})$) in Eqs.(19) and (20) are given by [17,18]:

$$\rho_{pr}(r) = \frac{1}{\left(\sqrt{\pi}a_{pr}\right)^3} e^{\left(\frac{-r^2}{a_{pr}^2}\right)} \quad (21)$$

and

$$\rho_{neu}(r) = \frac{1}{(\pi r_i^2)^{3/2}}\sum_{1}^{2}\theta_i\, e^{-r^2/r_i^2} \quad (22)$$

the parameters a_{pr}, θ_i and r_i are chosen so as to regenerate the experimental rms charge radii of the single proton and neutron, where $a_{pr} = 0.65\ fm$.
The values of θ_i and r_i are given in Table 1.

Table 1: The parameters of θ_i and r_i [18]

θ_1	1
θ_2	-1
r_1^2 (fm^2)	0.469
r_2^2 (fm^2)	0.546

The size radii (rms proton, neutron, charge and matter) are evaluated [17]:

$$\langle r^2\rangle_g^{\frac{1}{2}} = \sqrt{\frac{4\pi}{g}\int_0^\infty \rho_g(r) r^4 dr} \quad (23)$$

In Eq. (23) g stands for the proton, neutron, charge and matter.
Finally, the charge form factors in the plane-wave Born approximation is given by [17]:

$$F_{ch}(q) = \frac{4\pi}{qZ}\int_0^\infty \rho_{ch}(r)\sin(qr)\, r dr \quad (24)$$

where q and Z represent the momentum transferred to the nucleus from incident electrons and the atomic number of the target nucleus, respectively.

Results and Discussion

The calculations in the present work are based on the nuclear shell model in the independent particle motion; the core parts for all nuclei under study, (^{4,6,8}He) and (^{27,31}P), are investigated using harmonic-oscillator potential, while the valance parts are studied through Hulthen potential. Since there is no analytic solution for such mean field except for the s-states, the 1s state is chosen for the valence parts. Such treatment is symbolized by HO+H and used to investigate the root mean square proton, neutron, charge and matter radii, corresponding to density distributions and charge form factors.

In Table 1, the J^{π}(total spin and parity), the $t_{1/2}$ (half-life time), b_c (HO size parameters for protons and neutrons in the core), the κ_{t_z}(attenuation parameter for proton and neutron) and the experimental binding energy for single protons and neutrons on Fermi's level are presented. The attenuation parameter for proton and neutron (κ_{t_z}) were calculated from Eq. (10) using experimental binding energies for single proton (S_p) and neutron (S_n). The parameters $b_{c,n}$and $b_{c,p}$ were adjusted so as to regenerate the experimental size radii for the nuclei under study.

The calculated rms charge $\langle r^2\rangle_{ch}^{1/2}$, proton $\langle r^2\rangle_{p}^{1/2}$, neutron $\langle r^2\rangle_{n}^{1/2}$ and matter $\langle r^2\rangle_{m}^{1/2}$ radii for (^{4,6,8}He) and (^{27,31}P) are shown in Table 2. It is obvious that the calculations, in general, are in very good agreement with experimental data (^{4,6,8}He) and (^{27,31}P).
The calculated charge density distributions for stable ^{4}He and ^{31}P nuclei are portrayed in Figures 1 (a) and (b). It is clear from the figures that there is an overestimation in the central region in the calculations for ^{4}He and an underestimation for ^{31}P. The computed charge form factors for electron scattering for ^{4}He and ^{31}P are depicted in Figures 1 (c) and (d). It is worth noting that there is a very good prediction for the first diffraction minimum for ^{4}He and the first and second diffraction minima for ^{31}P. The calculations, in general, are in very good agreement with the data.

The calculated MDDs (matter density distributions) for ^{6}He, ^{8}He and ^{27}P are drawn in Figure 2 (a), (b) and (c) correspondingly. The solid curves show the theoretical calculations using the radial wave functions of HO and Hulthen potentials and this is represented by HO+Hulthen. The Shaded areas denote the empirical data taken from Ref [30] for ^{6}He, Ref. [31] for ^{8}He and Ref. [26] for ^{27}P. Unlike ^{6}He and ^{8}He, the κ_p for ^{27}p using $S_p = 0.807 \pm 0.009\ MeV$ is overestimates the calculation, therefore an adjustable parameter is used, $S_p = 2.4$ to predict the experimental data. It is obvious from the calculations that there is a very good agreement with experimental data were the long tail characteristic which is the remarkable feature of halo nuclei are well produced.

For helium and phosphorate isotopes, the computed MDDs are depicted in Figures 3 (a) and (b). It is clear from Figure 3 (a) that the long tail behavior for ^{6}He and ^{8}He is greatly distinguished from that of ^{4}He due to the low binding energies for the last neutron leading to such a long tail and indicating the halo formation for both isotope ^{6}He and ^{8}He. In Figure 3 (b), the low binding energy for the last proton resulted in a long tail in the MDD for ^{27}P, confirming the halo characteristic in such isotope.

In Figures 4 (a) and (b), the calculated Coulomb form factors for (^{4,6,8}He) and (^{27,31}P) nuclei are shown. For (^{4,6,8}He), it is worth noting that with increasing neutron number, the charge form factors shifted downwards and backwards, leading to the reduction in the electromagnetic interaction during the scattering process due to the screening effect. For (^{27,31}P), it is clear that with increasing proton number, the calculated charge form factor shifted forwards and upwards, indicating the enhancement in the scattering process due to the excess Coulomb interaction.

Table 2: $J^{\pi}T$, $t_{1/2}$, $b_{c,n}$, $b_{c,p}$, κ_n ,κ_p , S_p and S_n for Helium (^{4,6,8}He) and Phosphorate (^{27,31}P) isotopes

$^{A}_{Z}X_N(J^{\pi}T)$ [19]	$t_{\frac{1}{2}}(ms)$ [19]	$b_{c,n}$and $b_{c,p}$	κ_n and κ_p	Exp. Neutron binding energy (MeV) [20]	Exp. Proton binding energy (MeV) [20]
$^{4}_{2}He\ (0^{+}0)$	stable	$b_{c,n} = 1.3$ $b_{c,p} = 1.055$	κ_n =0.847 κ_p =0.311	S_n = 20.5776211(5)	S_p = 19.8138661(2)
$^{6}_{2}He\ (0^{+}1)$	806.92 ±0.00024	$b_{c,n} = 1.79$ $b_{c,p} = 1.607$	κ_n = 0.332	S_n = 1.7104569 ±0.0200001	S_p = 22.589323 ±0.0894427
$^{8}_{2}He\ (0^{+}2)$	119.5 ±0.0015	$b_{c,n} = 1.83$ $b_{c,p} = 1.513$	κ_n = 0.327	S_n = 2.5347627 ±0.00756	S_p = 24.814 ±1.004
$^{27}_{15}P\ \left(\frac{1^{+}}{2}\ \frac{3}{2}\right)$	260 ±0.08	$b_{c,n} = 1.688$ $b_{c,p} = 1.775$	κ_p = 0.334	S_n = 19.703 ±0.196	S_p = 0.8070001 ±0.009
$^{31}_{15}P\ \left(\frac{1^{+}}{2}\ \frac{1}{2}\right)$	stable	$b_{c,n} = 1.9$ $b_{c,p} = 1.85$	κ_n = 0.758 κ_p = 0.708	S_n = 12.3110066 ±0.0000652	S_p = 7.2965531 ±0.0000216

Table 3: Computed and empirical *rms* charge, proton, neutron and matter radii for Helium (^{4,6,8}He) and Phosphorate (^{27,31}P)

$^{A}_{Z}X_N(J^{\pi}T)$ [19]	Calculate $\langle r^2\rangle_p^{1/2}$	Exp. $\langle r^2\rangle_p^{\frac{1}{2}}$	Calculate $\langle r^2\rangle_m^{1/2}$	Exp. $\langle r^2\rangle_m^{1/2}$	Calculate $\langle r^2\rangle_{ch}^{1/2}$	Exp. $\langle r^2\rangle_{ch}^{1/2}$	Calculate $\langle r^2\rangle_n^{1/2}$	Exp. $\langle r^2\rangle_n^{1/2}$
^{4}He	1.508	1.57 ± 0.04 [21]	1.593	1.57 ± 0.04[21]	1.671	1.676 ± 0.008 [22]	1.673	1.67 ± 0.09[23]
^{6}He	1.968	2.21 ± 0.03 [21]	2.428	2.48 ± 0.03[21]	2.068	2.068 ± 0.01 [24]	2.628	2.61 ± 0.03[21]
^{8}He	1.853	-	2.601	2.58 ± 0.02[23]	1.929	1.929 ± 0.026 [24]	2.807	2.81 ± 0.03[25]
^{27}P	3.218	3.22 ± 0.163[26]	3.022	3.02 ± 0.155 [26]	3.290	-	2.756	2.754 ± 0.14[26]
^{31}P	3.106	-	3.146	-	3.187	3.187 ± 0.011 [22]	3.184	-

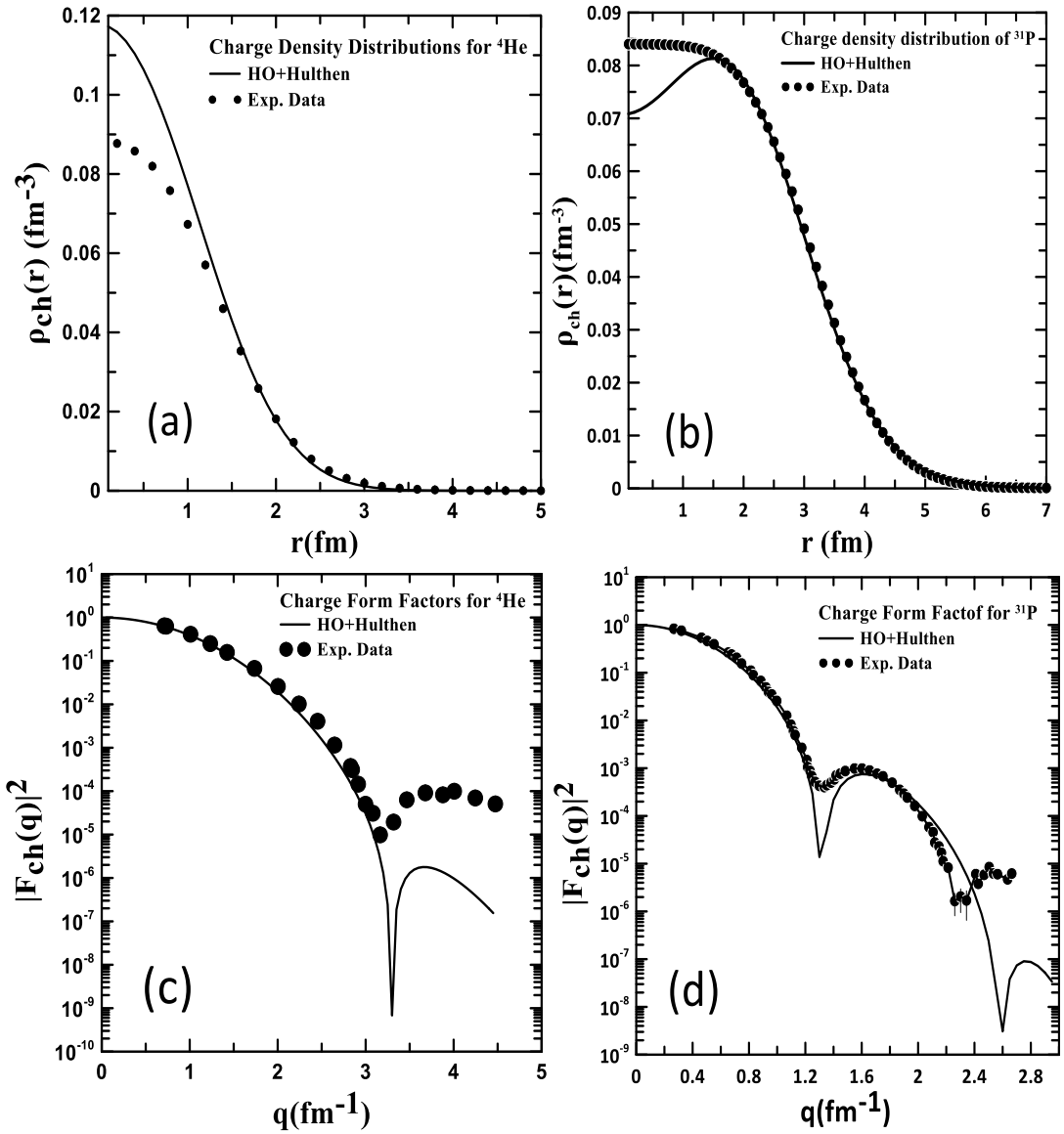

Figure 1: (a), (b), (c) and (d) represent the calculated CDDs and charge form factors for ^{4}He and ^{31}P nuclei, respectively. The theoretical calculation indicated by solid curves. The dotted curves represent experimental data. The experimental data for CDDs for both nuclei are taken from Ref. [22] while the experimental charge form factor are taken from Ref. [27, 28] for ^{4}He and Ref. [29] for ^{31}P.

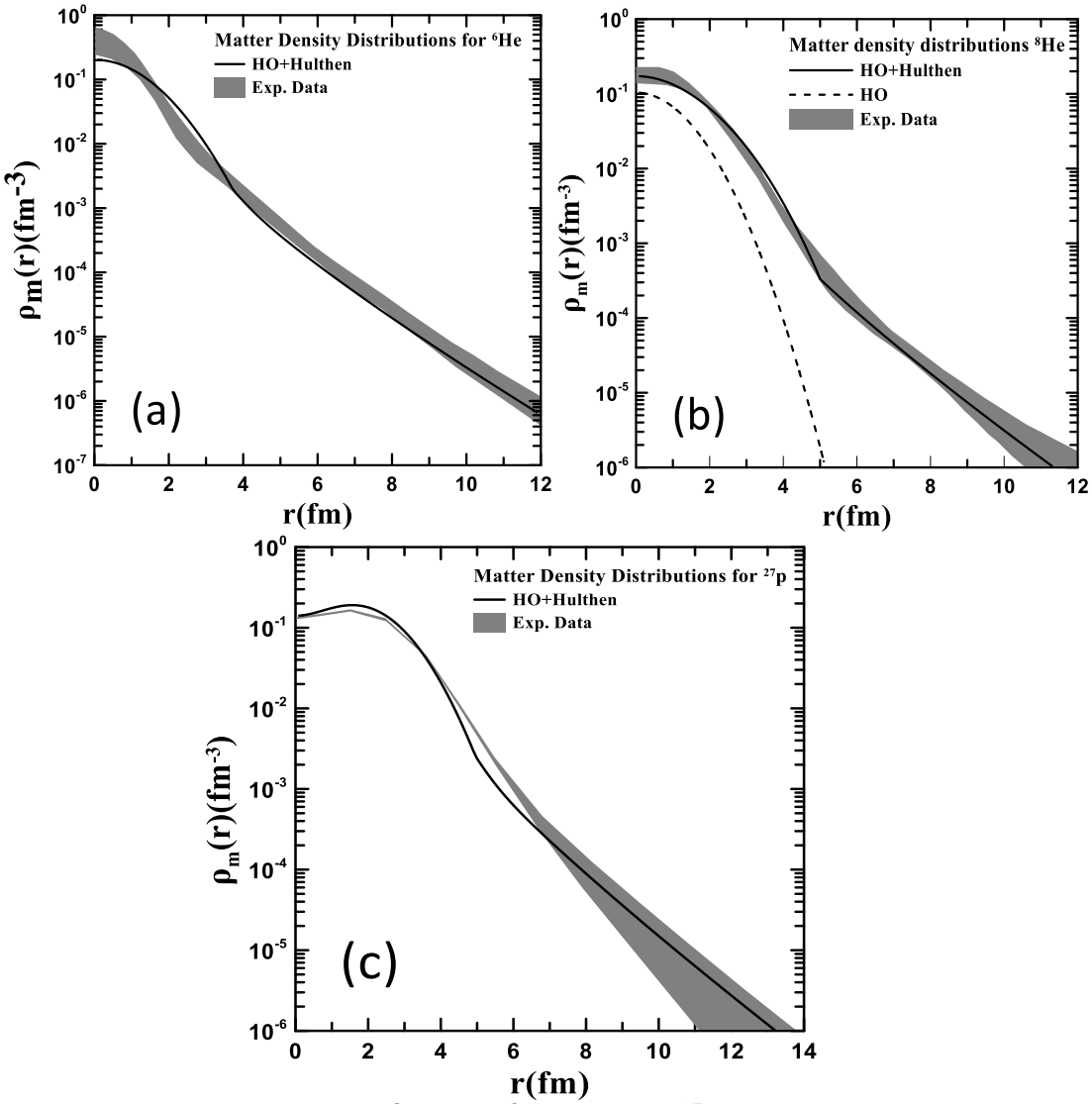

Figure 2: Calculated MDDs for ^{6}He (a), ^{8}He (b) and ^{27}P (c). The solid curves represent theoretical calculation. The shaded area represent experimental data taken from Ref [30] for ^{6}He, Ref. [31] for ^{8}He and Ref. [26] for ^{27}P.

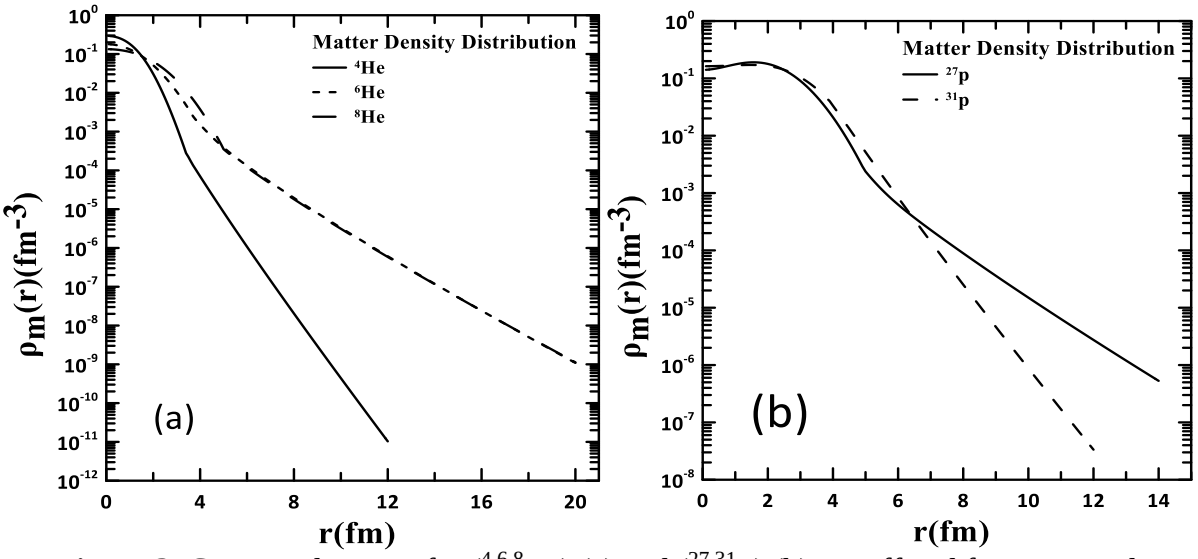

Figure 3: Computed MDDs for (^{4,6,8}He) (a) and (^{27,31}P) (b) are offered for compared.

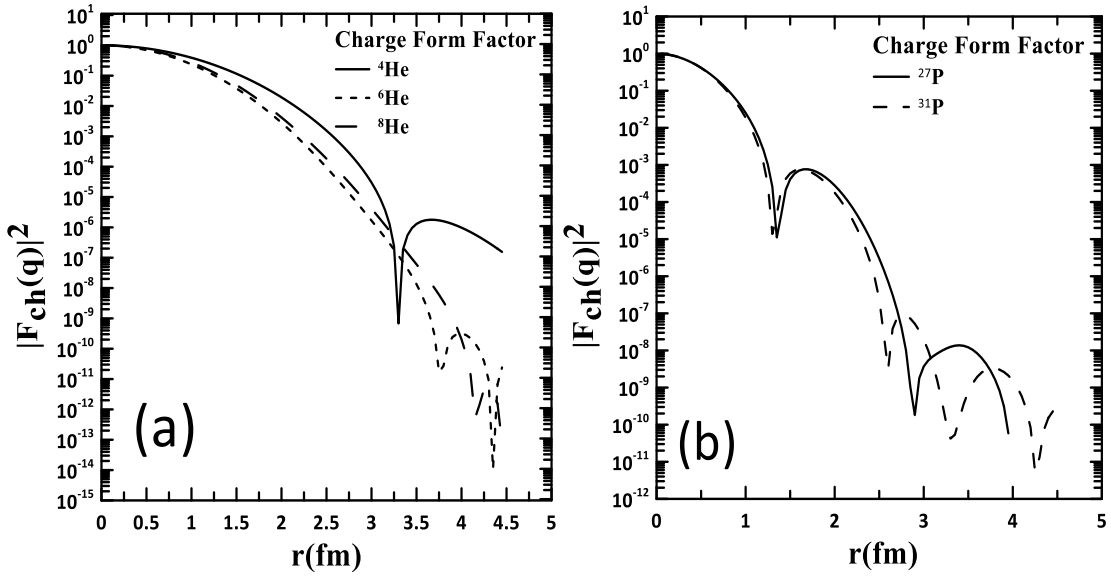

Figure 4: Calculated charge form factors for (^{4,6,8}He) (a) and (^{27,31}P) (b) are clarified.

Conclusions

It is concluded that the adoption of the radial WF of Hulthen potential are acceptable and gives very good results for the computation of size radii, density distributions and elastic charge form factors for Helium (^{4,6,8}He) and Phosphorate (^{27,31}P) isotopes. It was found that the increase in the core radius (matching point between HO and Hulthen) leads to increase in the calculated rms radii. The calculated CDD for ^{4}He overestimated the empirical data at central region, while there was an underestimation in the calculations for ^{31}P nucleus. At medium and large r, the agreement with experimental data were very good for both ^{4}He and ^{31}P nuclei. For the calculated matter density distributions, it is worth noting that the decrease in the binding energy for the valence nucleon(s) led to the remarkable upwards shift in the tail; this is ascribed to the excess in the tunneling effect. Finally, there was a backwards and downwards shifts for the calculated ground state charge form factors. This is attributed to the excess in the screening effect due to the increase in the neutron number leading to reduction in the scattering.

References

[1] C. J. Batty, E. Friedman, H. J. Gils and H. Rebel, "Advances in Nuclear Physics," vol. 19, pp. 1-188, 1989.

[2] E. William Hornyak, "Nuclear Structure," *Academic Press* , 1975.

[3] P. Navrátil, W. E. Ormand, E. Caurier and C. Bertulani, "Reaction mechanisim for rare Isotopes beams," *AIP Conference Proceedings* , vol. 791, no. 1, 2005.

[4] AK. Hamoudi, MA. Hasan and AR. Ridha. Pramana, "Nucleon momentum distributions and elastic electron scattering form factors for some 1p-shell nuclei," *Indian Academy of Sciences* , vol. 78, no. 5, pp. 737–748, 2012.

[5] AR. Radhi, AR. Ridha and WZ. Majeed, "Comparison between shell model and self-consistent mean field calculations for ground charge density distributions and elastic form factors of ^{12}C and ^{16}O nuclei," *Indian Journal of physics* , vol. 89, no. 7, pp. 723-728, 2015.

[6] K. Adel Hamoudi, A. Raad Radhi, R. Arkan Ridha, "Theoretical study of matter density distribution and elastic electron scattering form factors for the neutron-rich 22C exotic nucleus," *Iraqi Journal of Physics* , vol. 10, no. 19, PP. 25-34, 2012.

[7] R. A. Radhi, A. K. Hamoudi and A. R. Ridha, "Elastic Electron Scattering From Unstable Neutron- Rich ^{19}C Exotic Nucleus," *Iraqi Journal of Science* , vol. 54, no. 2, pp. 324-332, 2013.
[8] R. Arkan Ridha, K. Mustafa Suhayeb, "Theoretical Study of Nuclear Density Distributions and Elastic Electron Scattering form Factors for Some Halo Nuclei," *Iraqi Journal of Physics* , vol. 58, no. 4B, pp. 2098-2106, 2017.
[9] H. Saja Mohammed and R. Arkan Ridha, "Study of nuclear structure for carbon isotopes using local scale transformation technique in shell model," *Iraqi Journal of Physics* , vol. 16, no. 39, pp. 103-116, 2018.
[10] R. Arkan Ridha, "Study of charge density distributions elastic charge form factors and root-mean square radii for ^{4}He, ^{12}C and ^{16}O nuclei using WoodsSaxon and harmonic-oscillator potentials," *Iraqi Journal of Physics (IJP)* , vol. 14, no. 30, pp. 42-50, 2016.
[11] Rafah Ismail Noori and R. Arkan Ridha, "Density Distributions and Elastic Electron Scattering Form Factors of Proton-rich 8B, 17F, 17Ne, 23Al and 27P Nuclei," *Iraqi Journal of Physics* , vol. 17, no. 43, pp. 1-10, 2019.
[12] KG Heyde, "The Nuclear Shell Model," *verlag Berlin Heidelberg* , 1994.
[13] G. Roger Newton, "Scattering Theory of Waves and Particles," *McGraw-Hill, New York* , pp. 282, 1966.
[14] A. Laid, J. A. Tostevin and R. C. Johanson, "Deuteron breakup effects in transfer reactions using a Weinberg state expansion method," *PHYSICAL REVIEW C* , vol. 48 no. 3, pp. 1307-1317,1993.
[15] P. J. Von Brussard and P. W. M. Glaudemans, *North-Holland, Amesterdam* , 1977.
[16] R. A. Radhi, A. R. Ridha and W. Z. Majeed, "Comparison between shell model and self-consistent mean field calculations for ground charge density distributions and elastic form factors of ^{12}C and ^{16}O nuclei," *Indian Journal of physics* , vol. 89, no. 7, pp. 723-728, 2015.
[17] L. R. B. Elton, *Oxford University Press* , vol. 134, no. 3496, pp. 2092-2093, 1961.
[18] Harish Chandra and Gerhard Sauer, "Relativistic corrections to the elastic electron scattering from 208Pb," *Phys. Rev C* , vol. 13, no. 1, pp. 245-252, 1975.
[19] G. Audi, F. G. Kondev, W. J. Huang, and S. Naimi. "The NUBASE2016 evaluation of nuclear properties," *Chinese Physics C* , vol. 41, no. 3, pp. 1-138, 2017.
[20] F. G. Kondev, M. Wang, W. J. Huang, S. Naimi and G. Audi, "The NUBASE2020 evaluation of nuclear physics properties," *Chinese Physics C* , vol. 45, no. 3, pp. 1-180, 2021.
[21] I. Tanihata, T. Kobayashi, O. Yamakawa, S. Shimoura, K. Ekuni, K. Sugimoto, N. Takahashi, T. Shimoda and H. Sat, "Measurement of interaction cross section using isotopes beams of Be and B and isospin dependence of the nuclear radii," *Physics Letters B* , vol. 206, no. 4, pp. 592-596, 1988.
[22] H. DE VRIES, C. W. DE JAGER and C. DE VRIES, "Nuclear charge-density-distribution parameters from elastic electron scattering," *Atomic data and nuclear data tables* , vol. 36, no. 3, pp. 495-536, 1987.
[23] Suhel Ahmad, A. A. Usmani and Z. A. Khan, "Matter radii of light proton-rich and neutron-rich nuclear isotopes," *Physical Review C* , vol. 96, no. 6, pp. 1-13, 2017.
[24] Isao Tanihata, Herve Savajols, Rituparna Kanungo, "Recent experimental progress in nuclear halo structure studies," *Progress in Particle and Nuclear Physics* , vol. 68, no. 1, pp. 215-313, 2013.
[25] I. Tanihata, H. Hamagaki, O. Hashimoto, Y. Shida and N. Yoshikawa, "Measurements of Interaction Cross Sections and Nuclear Radii in the Light p-Shell Region," *Physical Review Letters* , vol. 55, no. 24, pp. 2676-2679, 1987.
[26] H. Y. Zhang, W. Q. Shen, Z. Z. Ren, Y. G. Ma, W. Z. Jiang, Z. Y. Zhu, X. Z. Cai, D. Q. Fang, C.
[27] Zhong, L. P. Yu, Y. B.Wei, W. L. Zhan, Z. Y. Guo, G. Q. Xiao, J. S. Wang, J. C. Wang, Q. J. Wang, J. X. Li, M. Wang and Z. Q. Chen, "Measurement of reaction cross section for proton-rich nuclei (A<30) at intermediate energies," *Nuclear Physics A* , vol. 707, pp. 303–324, 2002.
[28] R. Frosch, "Shell model analysis of elastic e^{-}-^{4}He scattering," *Phys. Lett. B* , vol. 37, pp. 140-142, 1971.
[29] R. G. Arnold, B. T. Chertok, S. Rock, W. P. Schütz, Z. M. Szalata, D. Day, J. S. McCarthy, F. Martin, B. A. Mecking, I. Sick and G. Tamas, "Elastic Electron Scattering from 3He and 4He at
[30] High Momentum Transfer," *Phys. Rev. Lett.* , vol. 40, no. 22, pp. 1429- 1432, 1978.
B. B. P. Sinha, G. A. Peterson, G. C Li. and R. R. Whitney, "Nuclear Charge Distributions of

Isotone Pairs. I. 31P and 32S," *Phys. Rev C*, vol. 6, pp. 1657-1663, 1972.

[31] M. Takechi, M. Fukudaf, M. Mihara, R. Matsumiya, K. Matsutaf, T. Minamisono, T. Ohtsubo, T. Izumikawa, S. Momota, T. Suzuki, T. Yamaguchil, S. Nakajima, K.

[32] Kobayashi, K. Tanaka, T. Suda, S. Sato, M. Kanazawa and A. Kitagawa. A. "Precise Studies of Nucleon Density Distribution of 6He and 8He," *American Institute of Physics Conference Proceedings*, vol. 891, pp. 187–191, 2007.

[33] Masaomi TANAKA, Mitsunori FUKUDA, Daiki NISHIMURA, Shinji SUZUKI, Maya TAKECHI, Mototsugu MIHARA, Kensaku MATSUTA, Yusuke MORITA, Yasuto KAMISHO, Junichi OHNO, Ryosuke KANBE, Shintaro YAMAOK, Kota WATANABE, Takashi OHTSUBO, Takuji IZUMIKAWA, Masayuki NAGASHIMA, Akira HONMA, Daiki MUROOKA, Takashi SUZUKI, Takayuki YAMAGUCHI, Junpei KOHNO, Sayaka YAMAKI, Satoshi MATSUNAGA, Shunpei KINNO, Yoshimasa TAGUCHI, Atsushi KITAGAWA, Shigekazu FUKUDA, and Shinji SATO. "Reaction cross sections for 8He and 14B on proton target for the separation of proton and neutron density distributions, " JPS Conf. Proc, vol. 6, pp. 1-6, 2015